Proc. Indian Acad. Sci. (Earth Planet. Sci.), Vol. 94, No. 3, November 1985, pp. 261–267.

HF doppler observations on the occurrence of equatorial spread-F

B T VIKRAM KUMAR, P VELAYUDHAN NAIR and P B RAO
Department of Physics, University of Kerala, Kariavattom, Trivandrum 695 581, India

MS received 15 March 1985; revised 5 July 1985

Abstract. HF doppler observations of the vertical drift velocity and group height of the 5·5 MHz plasma frequency level of the post-sunset bottomside F-region obtained on a few ESF (equatorial spread-F) and non-ESF days at Trivandrum are presented. The results show that on the non-ESF days, the maximum group height attained is about 400 km and the maximum velocity is less than 30 m/sec. On the ESF days, however, the corresponding values are found to be in the range of 400–650 km and 30–50 m/sec. The ESF onset is found to be significantly delayed relative to the velocity peak indicating that it is more closely linked to the layer height than to the drift velocity.

Keywords. HF doppler observations; vertical shift velocity; group height; equatorial spread-F; drift velocity; layer height.

1. Introduction

The occurrence of equatorial spread-F (ESF) has been known for long, but significant advancement in the understanding of the phenomenon has been made only in recent years. The current understanding of ESF has come about through a variety of observational techniques as well as theoretical and computer simulation studies (for reviews, see: Basu and Kelley 1979; Fejer and Kelley 1980; Ossakow 1981). The basic process involving the operation of a hierarchy of instability mechanisms, which could account for most of the observed ESF characteristics, have been successfully identified. According to the current picture, ESF onset is believed to occur via the collisional Rayleigh-Taylor instability mechanism operating on the steep electron density gradient in the bottomside F-region when its altitude is high enough to overcome the recombination effects. Using VHF radar observations at Jicamarca, Farley *et al* (1970) have found that there is an altitude threshold of about 350 km for the bottom side (0·01 N_{max} level) for ESF onset to occur. The linear growth rate for the instability given by Ossakow *et al* (1979) indicates that an eastward electric field might also contribute in a significant way to the onset of ESF. Some indirect evidence that the growth rate of irregularities is governed initially by the background electric field is presented by Rastogi and Woodman (1978). Another important consequence of the background electric field is that it contributes significantly to the polarization of the plasma depletions (bubbles) which determines their vertical rise velocity (Anderson and Haerendel 1979). In this paper, we present some HF doppler observations on the vertical drift velocity and group height of the post-sunset bottomside F-region obtained during a few ESF and on non-ESF days at Trivandrum (dip: 56′ S). The results are used to examine the association of the two parameters with the onset of ESF.

2. Description of the experimental technique

The HF doppler radar consists of a pulse transmitter, a phase coherent receiver, the associated antennas and recording units. The block diagram of the system is given in figure 1. All the frequencies required for the system are generated by a master frequency synthesizer which has a long term frequency stability of better than one part in 10^7. A 5·5 MHz r.f. wave is modulated by a transmitter pulse having a pulse width of 100 μsec and a PRF of 50 Hz, in the modulator unit. The resulting modulated r.f. pulse is fed to the transmitter, in which the pulse undergoes various stages of amplification. The final output is a pulse of 3 kW peak power, which is fed to the 600 Ω folded dipole transmitting antenna through 600 Ω transmission lines.

The receiving system is shown in figure 2. The vertically transmitted signal gets reflected from the ionosphere and is received by a half-wave dipole, which is connected to the receiver through a coaxial cable. The received signal frequency is 5·5 MHz $\pm \Delta f$, where Δf is the doppler frequency. At the receiver input, it is mixed with a 5 MHz signal and the resulting 500 KHz $\pm \Delta f$ is amplified by the tuned IF amplifier. Now, for the second mixer, a 2 MHz signal from the frequency synthesizer is divided and phase-shifted so as to provide two phase quadrature local oscillator frequencies of 500 KHz. The amplified signal from the IF stage is mixed with each of these 500 kHz to obtain quadrature outputs at the doppler frequency of $\pm \Delta f$. Each of these quadrature outputs is passed through a balanced to unbalanced amplifier, a low-pass butterworth filter, and a sample and hold circuit. The sampling gate pulse is of 10 μsec duration and it occurs at the same rate as the transmitter PRF with a delay that can be varied over the inter-pulse period. The sampling circuit is followed by a FET-input operational amplifier operating as a voltage follower. These stages are identical for both the

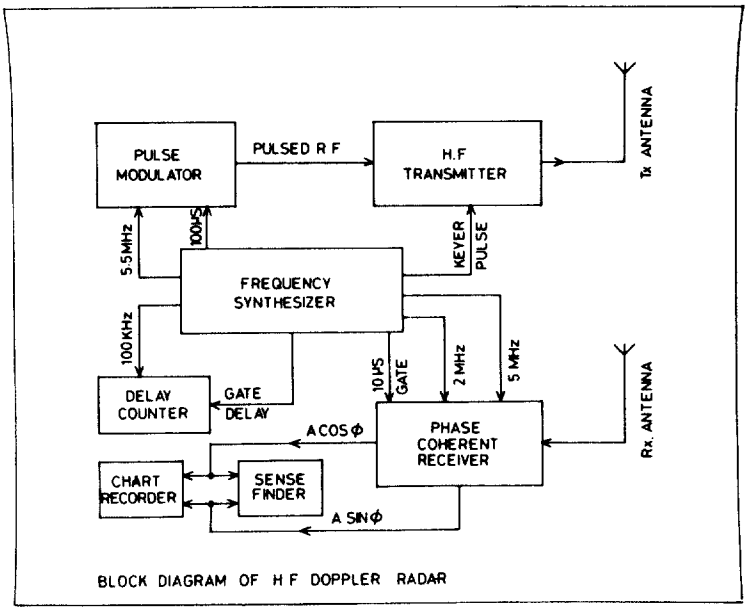

Figure 1. Block diagram of the HF doppler system.

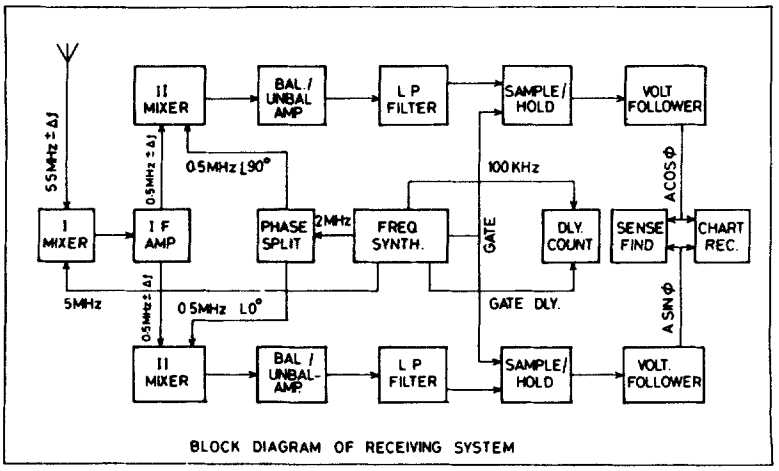

Figure 2. Block diagram of the phase coherent receiving system.

quadrature channels, termed as "cos" and "sin" channels. The final outputs from the receiver are slowly varying d.c., which are fed to a multi-channel stripchart recorder as well as to a sense detector, which resolves the sign of the doppler. The gate-delay pulse from the synthesizer is fed to a delay counter which counts and displays the delay with a resolution of 10 μsec. The chart recorder is normally run at a speed of 10 cm/min. Using this chart speed, it is possible to measure the doppler in the range 0 to $\pm 2{\cdot}5$ Hz, which corresponds to a vertical velocity range of about 0 to ± 70 m/sec. The uncertainties associated with the chart scaling are such that the doppler and hence the vertical drift velocity can be measured to an accuracy better than 2%.

Some sample records of the ionospheric signal on an ESF day are shown in figure 3. The sample records shown are for different time periods, before the onset of ESF, during ESF, and after ESF has disappeared. It can be seen that there is a rapid variation in doppler with time and the corresponding vertical drift velocities for the five sample times are: (a) 6 m/sec, (b) 16 m/sec, (c) 41 m/sec, (d) 15 m/sec and (e) 0·8 m/sec.

3. Observations and results

For the present observations, aimed at studying the conditions of occurrence of ESF, the system was operated in the evening from 1700 IST to the time when the critical frequency falls below the operating frequency, which occurs between midnight and 0300 IST. The doppler and group delay were recorded every five minutes. During ESF, range gating of the signal is very difficult due to the broadening of the returned pulse and the presence of multiple echoes. In such cases, the gate is kept at the strongest of the echoes, and from the records we judge that an uncertainty of about 30 km is possible in group height. Ten days of data are presented here, of which, five days are ESF days. The doppler frequency is converted to the vertical velocity of the layer. The derived drift velocity is to be regarded in the strict sense, as apparent as it includes also the contribution due to the decay of the layer. However, it is found from an exercise carried out on an exponentially decaying parabolic profile following Budden (1961), with

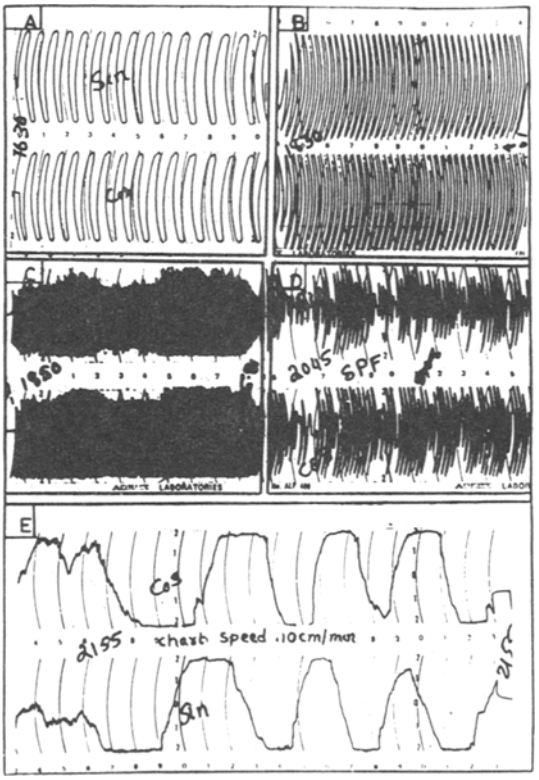

Figure 3. Sample doppler records of ionospheric signal on 15 March 1984, an ESF day. The first four panels represent data recorded for one minute with starting time: **A)** 1630 IST, **B)** 1830 IST, **C)** 1850 IST, **D)** 2045 IST, panel **(E)** represents data for two minutes starting at 2155 IST. Only panel **(D)** represents data during ESF. The chart speed is 10 cm/min for all records.

appropriate equatorial parameters, that the contribution due to decay doppler is in the range of about 5–20% during the period of interest to the current study. The higher values of decay doppler occur for short periods immediately following sunset and also later in the night when the operating frequency approaches the critical frequency. The decay doppler, however, is not expected to affect the results of the study seriously since its contribution is present on both ESF and non-ESF days to the same extent. The derived drift velocity may, therefore, be considered to represent essentially the true vertical drift of the 5·5 MHz plasma frequency level. A similar calculation on the group height shows that, in general, it is 50–100 km above the true height during the pre-midnight period of interest here. The time variations of both the drift velocity and the group height for all the ten days as well as their averages, obtained separately for the ESF and non-ESF days, are presented.

Figure 4 shows the time variations of the vertical drift and group height of the post-sunset F-region on different days. It can be seen that to start with, prior to sunset on all days, the velocity has a small positive value and the group height of the layer is in the range 300–350 km. The drift velocity starts to increase rapidly around 1800 hrs to reach

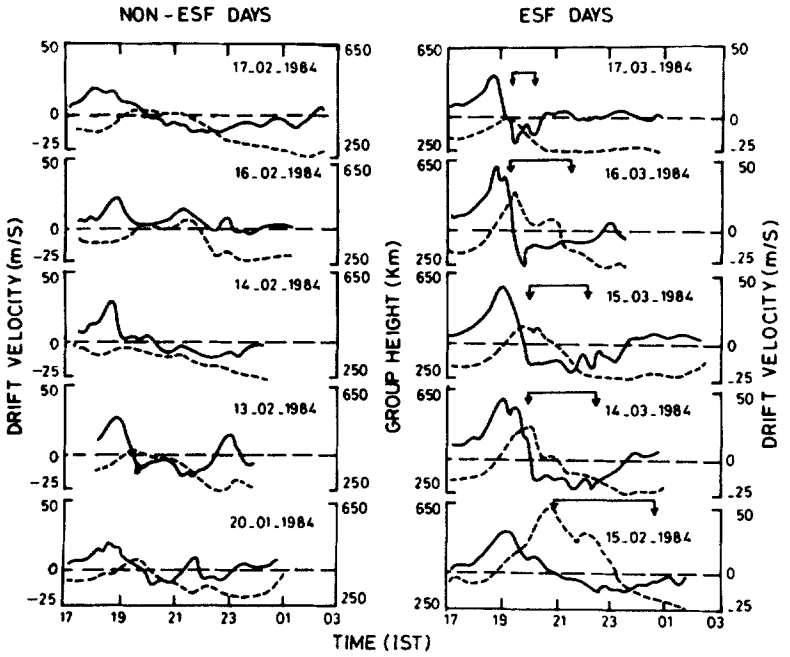

Figure 4. Time variations of drift velocity and group height on ESF and non-ESF days. (—— drift velocity; . . . . . group height). The arrow marks indicate the period when ESF is present.

a maximum around 1900 hrs and then decreases to cross zero and becomes negative by 2100 hrs. The group height also increases following sunset and reaches a maximum at about the same time when the drift velocity goes through the transition from positive to negative. It is clear that the variations are more rapid and of greater magnitude on ESF days than on non-ESF days. On the non-ESF days, the maximum group height attained is around 400 km and the maximum velocity is less than 30 m/sec. On the ESF days, however, the maximum group height is in the range of 400–650 km and the maximum velocity is in the range of 30–50 m/sec. The example of March 17, 1984 seems to represent a border-line case with regard to the conditions conducive for the onset of ESF. On this day, the maximum group height was about 400 km and the maximum drift velocity was about 30 m/sec. There was an occurrence of weak spread-F for a duration of about an hour. Another feature which may be noted from figure 4 is that, once spread-F has occurred, it will disappear only after the group height has decreased below about 300 km. This is to be expected since, when the layer descends to lower heights crossing a threshold, the recombination effects begin to dominate over the conditions favourable for sustaining the spread-F. Figure 5 presents an average picture of the time variations of the group height and the vertical drift velocity for the ESF and non-ESF days separately. The figure brings out the essential features which show that for non-ESF days, the maximum group height and the drift velocity are about 400 km and 25 m/sec respectively, whereas for ESF days the corresponding values are about 475 km and 40 m/sec.

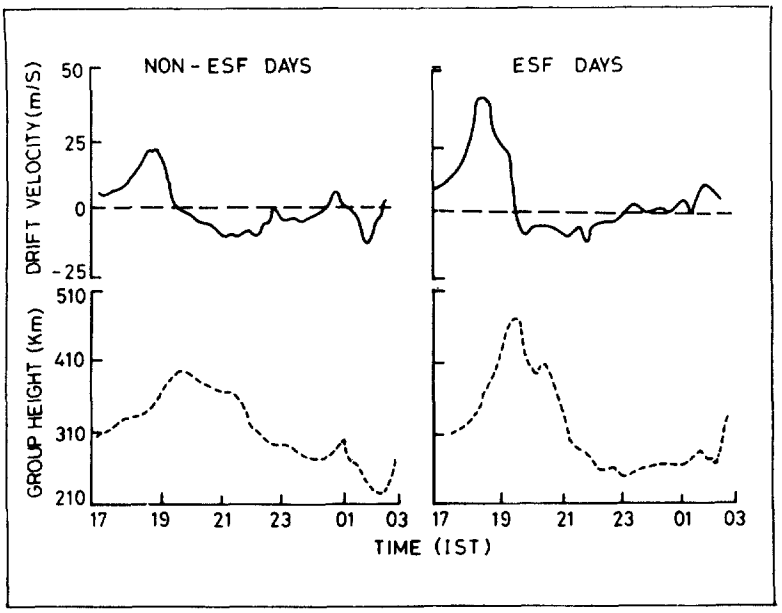

Figure 5. Average time variations of drift velocity and group height on ESF and non-ESF days (—— drift velocity; . . . . . group height).

4. Discussion

The association of the occurrence of ESF with the post-sunset height rise of the F-layer has been known for long. Using radar backscatter measurements, Farley *et al* (1970) have found an altitude threshold for the bottomside of the F-layer for the onset of ESF. They observed that the bottomside, where the plasma density drops to 1 % of that at the F-layer peak, must be above about 350 km for ESF onset to occur. The above radar observations indicating an altitude threshold seem to be consistent with the conditions favourable for the collisional drift instability advanced by Hudson and Kennel (1975) to account for the short wavelengths of the irregularity spectrum. In recent years, a clear picture has emerged on the processes leading to the presence of a wide range of scale sizes of irregularities observed during ESF. It involves the operation of a hierarchy of instabilities first suggested by Haerendel (1974) and later developed by many workers as reviewed by Ossakow (1981). The growth rate of the collisional Rayleigh-Taylor instability, which seems to indicate ESF in the bottomside, is given by Ossakow *et al* (1979) as:

$$r = (1/L)(g/\nu_{in} + CE/B) - \nu_R$$

where L is the electron density scale height, E is the eastward component of the electric field, ν_{in} is the ion-neutral collision frequency, ν_R is the recombination coefficient and g, B and C are the acceleration due to gravity, the magnetic field and the velocity of light respectively. It is known that due to recombination and possible electrodynamic effects, the bottomside F-region electron density gradient begins to steepen immediately

following sunset. Added to the steepening, if the altitude of the F-region is sufficiently high to overcome the recombination effects, plasma density fluctuations will begin to grow on the bottomside via the collisional Rayleigh-Taylor mechanism.

The post-sunset vertical drift velocity of the layer associated with the eastward electric field seldom exceeds 50 m/sec. That, this velocity alone is not enough to cause ESF onset is clear from figure 4 showing the onset to be significantly delayed relative to the velocity peak. The ESF onset, occurring around the same time as the peak of the group height, seems to depend more on the layer height than on the drift velocity, an observation consistent with that of Farley *et al* (1970). It has also been reported earlier by Chandra and Rastogi (1972a, b, 1978) that the maintenance of F-region at higher altitudes is an important condition for the occurrence of ESF. Their results have shown that on ESF days, drift reversals occur later than on non-ESF days suggesting that higher altitudes are attained for the F-region on ESF days. It may, however, be noted that high drift velocities cause the layer to rise to high altitudes and, therefore, a high drift velocity of the post sunset F-region may be taken as an indication that favourable conditions will be attained for the onset of ESF. It seems that if the drift velocity exceeds a value of about 30 m/sec, the layer will attain a high enough altitude to overcome the recombination effects for the density fluctuations to grow via the collisional Rayleigh-Taylor mechanism resulting in the onset of ESF. Another important consequence of the vertical drift velocity which is of interest to ESF is its possible contribution to the polarization of the plasma bubbles and hence to their vertical rise velocity (Anderson and Haerendel 1979). The results presented in figure 4, however, show that ESF onset as seen by the HF radar is well past the drift velocity peak indicating that the background electric field may not be contributing significantly to the plasma bubble polarization. In such a case, it is essentially the gravity-driven components which determine the polarization and the vertical rise velocity of the plasma bubbles.

Acknowledgements

The HF doppler system has been built under an ISRO sponsored RESPOND Project. We thank Dr N Balan and Mr N Sugunan for assistance.

References

Anderson D N and Haerendal G 1979 *J. Geophys. Res.* **84** 4251
Basu S and Kelley M C 1979 *Radio Sci.* **14** 471
Budden K G 1961 *Radio waves in the ionosphere* (London and New York: Cambridge Univ. Press) pp. 153
Chandra H and Rastogi R G 1972a *Ann. Geophys.* **28** 37
Chandra H and Rastogi R G 1972b *Ann. Geophys.* **28** 709
Chandra H and Rastogi R G 1978 *Indian J. Radio Space Phys.* 7 265
Farley D T, Balsley B B, Woodman R F and Mc Clure J P 1970 *J. Geophys. Res.* **75** 7199
Fejer B G and Kelley M C 1980 *Rev. Geophys. Space Phys.* **18** 401
Haerendal G 1974 Report, Max-Planck Inst. fur Phys. und Astrophys., FRG
Hudson M K and Kennel C F 1975 *J. Geophys. Res.* **80** 4581
Ossakow S L, Zalesak S T, Mc Donald B E and Chaturvedi P K 1979 *J. Geophys. Res.* **84** 17
Ossakow S L 1981 *J. Atmos. Terr. Phys.* **43** 437
Rastogi R G and Woodman R F 1978 *J. Atmos. Terr. Phys.* **40** 485